

# From itinerant to local transformation and critical point in Ni-rich $\text{Ce}_2(\text{Ni}_{1-y}\text{Pd}_y)_2\text{Sn}$

J.G. Sereni <sup>1</sup>, G. Schmerber <sup>2</sup>, M. Gómez Berisso <sup>1</sup> and J.P. Kappler <sup>2</sup>

<sup>1</sup>Low Temperature Div. CAB - CNEA, Conicet, 8400 Bariloche, Argentina and

<sup>2</sup>IPCMS, UMR 7504 CNRS-ULP, 23 rue de Loess, B.P. 43 Strasbourg Cedex 2, France

(Dated: November 26, 2021)

Structural, magnetic ( $M$ ) and thermal ( $C_m$ ) studies on  $\text{Ce}_2(\text{Ni}_{1-y}\text{Pd}_y)_2\text{Sn}$  alloys are presented within the  $0 \leq y \leq 0.55$  range of concentration, showing evidences for itinerant to local electronic transformation. At variance with RKKY type interactions between localized moments  $\mu_{eff}$ , the substitution of Ni by isoelectronic Pd leads the antiferromagnetic transition to decrease from  $T_N$  3.8 K to 1.2 K between  $y = 0$  and 0.48, while  $M(H)$  measured at  $H = 5$  T and 1.8 K rises from 0.12 up to  $0.75\mu_B/\text{Ce-at.}$  Furthermore, the  $C_m(T_N)$  jump increases with concentration whereas  $|\theta_P|$  decreases. The magnetic entropy  $S_m(T)$  grows moderately with temperature for  $y = 0$  due to a significant contribution of excited levels at low energy, while at  $y = 0.5$  it shows a incipient plateau around  $S_m = R\ln 2$ . All these features reflect the progressive ground state transformation of from itinerant to a local character.

Another peculiarity of this system is the nearly constant value of  $C_m(T_N)$  that ends in an *entropy bottleneck* as  $T_N$  decreases. Consequently, the system shows a critical point at  $y_{cr} \approx 0.48$  with signs of ferromagnetic behavior above  $H_{cr} \approx 0.3\text{ T}$ . A splitting of the  $C_m(T_N)$  maximum, tuned by field and concentration, indicates a competition between two magnetic phases, with respective peaks at  $T_N \approx 1.2\text{ K}$  and  $T_I \approx 1.45\text{ K}$ .

## I. INTRODUCTION

Itinerant magnetism is mostly observed in U or Pu-based compounds because of their  $5f$  orbitals [1] whereas a local character is mostly expected in  $4f$  Ce and Yb ones. However, one basic question, not fully elucidated yet, concerns the possibility of a local to itinerant transformation of the Ce- $4f^1$  orbital. This possibility was investigated for 30 years within the so called *local-itinerant dilemma* [2]. Although the  $4f^1$  delocalization is well documented among systems showing  $4f$  and conduction band hybridization [3], that mechanism implies the screening of the magnetic moment with the consequent weakening of the magnetic order. In spite of that, there are Ce compounds showing magnetic order with record high values, being the outstanding examples  $\text{CeRh}_3\text{B}_2$  ( $T_C = 115\text{ K}$  [4]),  $\text{CeScGe}$  ( $T_N = 47\text{ K}$  [5]) and  $\text{CeRh}_2\text{Si}_2$  ( $T_N = 36\text{ K}$  [6]), which are claimed to exhibit itinerant magnetism.

One characteristic of a well localized Ce- $4f$  orbital is related to the fact that the doublet ( $N = 2$ ) ground state (GS) is not significantly affected by Kondo screening ( $T_K$ ) and the excited crystal field (CEF) levels have a comparatively large splitting ( $\Delta_{CEF}$ ), i.e.  $T_K \ll \Delta_{CEF}$ . The opposite scenario, with  $T_K \geq \Delta_{CEF}$ , is the proper situation where to search for itinerant magnetic behavior provided that the magnetic order still occurs, which only occurs in a few system. As a consequence of an eventual  $N_{eff} > 2$  character, the magnetic contribution to the entropy ( $S_m$ ) is expected to overcome the  $R\ln 2$

value at relatively low temperature.

These conditions were recently observed in the ternary system  $\text{Ce}_2(\text{Pd}_{1-x}\text{Ni}_x)_2\text{Sn}$  [7]. There, the substitution of Pd atoms by isoelectronic Ni leads to a change from local (Pd-rich side) to itinerant (Ni-rich side) character. Such a change in the electronic structure is associated to a crystallographic modification from tetragonal  $\text{Mo}_2\text{FeB}_2$  to centered orthorhombic structure of  $\text{W}_2\text{CoB}_2$  type [8] between  $0.25 \leq y \leq 0.35$ , where a gap of miscibility occurs.

With the aim to compare the Ce- $4f$  orbital nature in these two phases, the magnetic properties of the  $\text{Ce}_2(\text{Ni}_{1-y}\text{Pd}_y)_2\text{Sn}$  alloys on the Ni-rich side (i.e. within the orthorhombic structure) were investigated. Apart from the usual magnetic characterization, for a proper analysis of the itinerant to localized evolution of the system we focus on the study of two basic parameters: the height of the specific heat anomaly at  $T = T_N$  and the thermal dependence of the entropy  $S_m(T)$ . These quantities allow to evaluate the role of the Kondo effect and how the excited CEF levels contribute to the ground state properties.

## II. EXPERIMENTAL RESULTS

### A. Magnetic Susceptibility

The high temperature magnetic behavior ( $T \geq 80\text{ K}$ ) is well described by a Curie-Weiss type contribution ( $\chi = C_C/(T - \theta_P)$ ) plus a minor Pauli

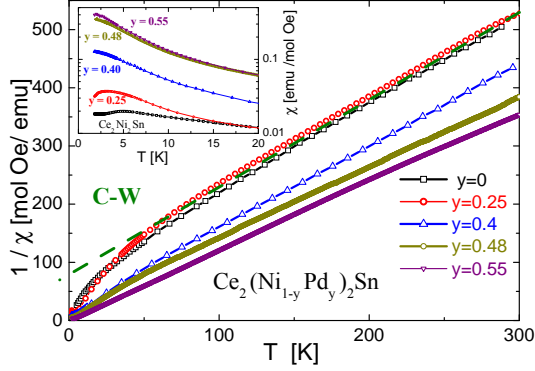


FIG. 1. High temperature inverse susceptibility of Ni-rich alloys measured with  $\mu_0 H = 0.1$  T. Inset: low temperature magnetic susceptibility in a logarithmic scale.

contribution ( $\chi_P = 5 \pm 2 \times 10^{-3}$  emu/mol Oe). In Fig. 1 the inverse of  $\chi$  is presented to extract the respective paramagnetic temperatures  $\theta_P(y)$  and effective moments  $\mu_{eff}(y) \propto \sqrt{C_C}$ . The  $\theta_P(y)$  values range between  $-58$  K at the Ni-rich limit and  $\approx 6$  at  $y = 0.55$ . Simultaneously,  $\mu_{eff}(y)$  increases from  $\mu_{eff} = 2.3\mu_B$  up to  $\approx 2.54\mu_B$  between those concentration values. A detail of the  $\chi(T)$  dependencies at low temperature ( $T < 20$  K) are included in the inset of Fig. 1 using a logarithmic scale to cover the large variation of  $\chi(y)$  at  $T = 1.8$  K.

In order to explore this strong increase of  $\chi(y)$  at low temperature the isothermal field dependence of the magnetization  $M(H)$  was measured at  $T = 1.8$  K, 3 K and 4 K up to  $\mu_0 H = 5$  Tesla. A clear difference in the  $M(H)$  dependence can be appreciated in the results obtained at  $T = 1.8$  K between Ni-rich samples and those with similar Pd/Ni concentration (see Fig. 2a). While  $M(H)$  shows a slight positive curvature with low values of  $M$  in  $y = 0$  ( $0.15\mu_B$ ) and 0.25 alloys, those with  $y \geq 0.4$  show a tendency to saturation ( $M_{sat}$ ) at  $H = 5$  Tesla. Despite the fact that the former alloys have a  $T_N \geq 1.8$  K while in the latter  $T_N < 1.8$  K, similar measurements performed at  $T = 4$  K (i.e. in the paramagnetic phase) show the same variation. Notably,  $M_{sat}(y)$  undergoes a maximum of  $0.88\mu_B$  at  $y = 0.40$  and then slightly decreases to  $0.76\mu_B$  for  $y = 0.55$ . In coincidence with the  $M_{sat}$  decrease at these concentrations, the initial slope of  $M(H)$  increases as a sign of a stronger interaction between magnetic moments. Additionally, a further slight increase in the slope is observed around  $H = 1$  Tesla. To remark these features, the  $\partial M/\partial H$  derivative is presented in Fig. 2b, showing that the change of slope only occurs in the

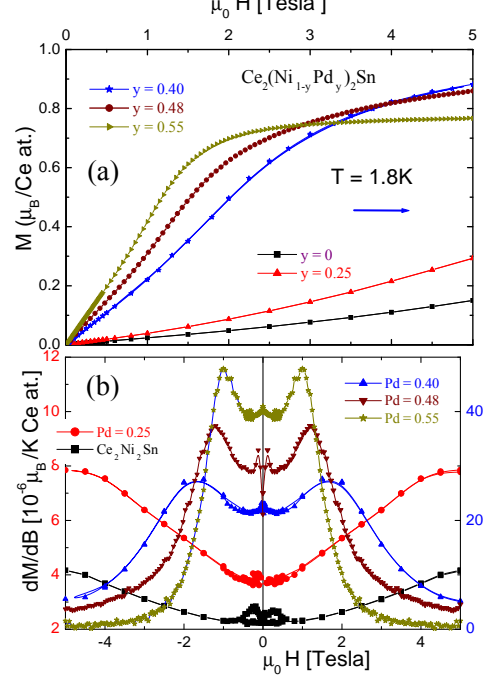


FIG. 2. a) Field dependent magnetization of the 1.8 K isotherms for the Ni-rich range measured up to 5 T. b)  $dM/dH$  vs  $H$  derivative showing the difference between Ni-rich samples (left axis) and those with similar Pd/Ni concentration (right axis).

alloys with strong magnetization (i.e.  $y \geq 0.4$ ) and it grows up to  $y = 0.55$ . Notably, the  $M(H)$  dependence above that critical field is properly described by a  $\tanh(H)$  function which characterizes ferromagnetic systems.

## B. Specific heat

The magnetic contribution ( $C_m$ ) to the measured ( $C_P$ ) specific heat was obtained by subtracting the phonon contribution extracted from the reference isotopic compound  $\text{La}_2\text{Ni}_2\text{Sn}$  as  $C_m = C_P - C_{La}$ . From the thermal dependence of  $C_m$  one can see in Fig. 3a that the ordering temperature  $T_N(y)$ , defined as the temperature of the maximum of  $C_m(T)$ , decreases with Pd concentration. This evolution extrapolates to  $T_N = 0$  at  $y \approx 0.70$ , beyond the structural stability of this system. However, between  $0.48 \leq y \leq 0.52$ ,  $T_N(y)$  remains nearly constant at  $T_N \approx 1.2$  K while another anomaly arises for  $y = 0.55$  at  $T_I \approx 1.5$  K as shown in Fig. 3b.

While the  $C_m(T)$  dependence at  $T < T_N$  is typical for an antiferromagnetic system, the  $C_m(T)$  maxi-

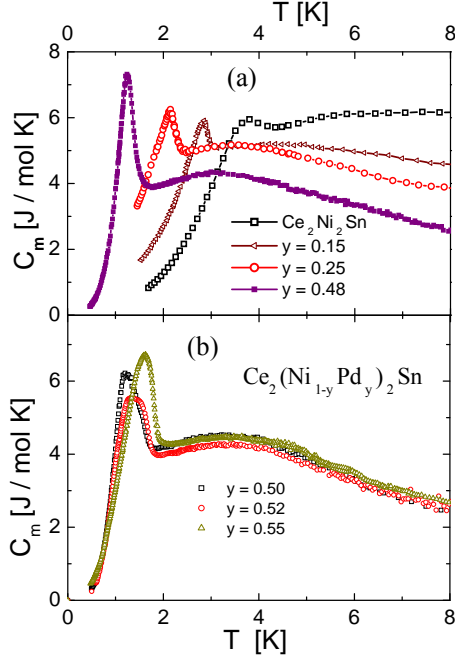


FIG. 3. Thermal dependence of the magnetic contribution to the specific heat  $C_m$  for: a) Ni-rich alloys and b) critical region at similar Ni/Pd concentration.

mum ( $C_{max}$ ) behaves quite unusual because its value slightly changes up to  $y = 0.48$  and becomes sharper as Pd concentration increases, see Fig. 3a. According to the law of corresponding states,  $C_{max}$  should decrease with decreasing  $T_N(y)$ , to become zero at  $T = 0$ . As a consequence the magnetic transition with chances to reach zero temperature have to show  $C_{max}/T_N \approx \text{const.}$  [9]. On the contrary, this system shows  $C_{max}/T$  rising as  $\propto 1/T_N(y)$  as indicated in Fig. 4a. This divergent  $C_{max}/T_N$  dependence places the  $y = 0.48$  alloy at a critical concentration point.

Above  $T_N(y)$ ,  $C_m(T)$  shows a very broad maximum which progressively decreases in temperature and intensity as Pd concentration increases, see Fig. 3. Such a temperature dependence is characteristic of non-Fermi-liquids (NFL) [10, 12] in the region of quantum critical behavior that affects the thermal properties because of emerging quantum fluctuations. These low energy fluctuations overcome classical thermal fluctuations below 2 or 3 K as it was observed in Ce NFL systems [11]. Within that regime, a characteristic  $C_m(T)/T = -A \log(T/T^*)$  thermal dependencies occurs, like the observed in this system above  $T_N$ , see Fig. 4. The parameter  $T^*$  represents a characteristic energy scale that describes the range of the  $C_m(T)/T$  tail. The obtained  $A$  and  $T^*$  pa-

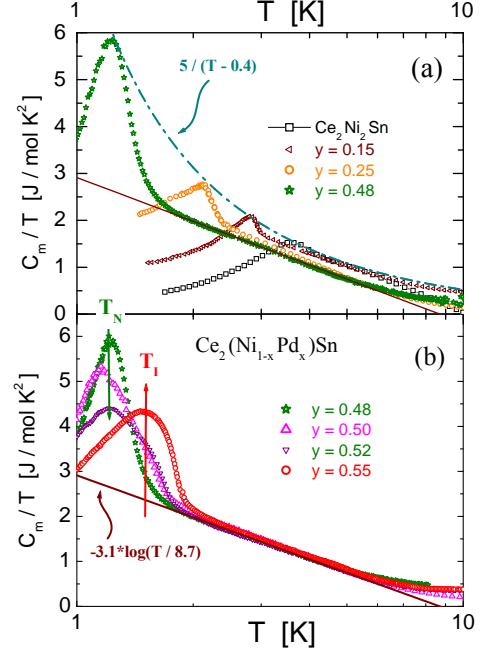


FIG. 4. Logarithmic dependence of the magnetic contribution to specific heat divided by temperature  $C_m/T$  for: (a)  $0 \leq y \leq 0.48$  samples. Dash-dot curve describes the  $C_m/T(y)$  maxima dependence. (b) Alloys with Pd/Ni equi-atomic concentrations. Arrows at  $T_N$  and  $T_I$  indicate a two phases competition. Straight line represents a logarithmic reference fitting a universal function (see the text).

rameters allow to scale this system into an universal curve  $C_m/t = -7.2 \log(t)$ , with  $t = T/T^*$ , extracted for a number of Ce intermetallic compounds showing logarithmic thermal dependencies [13].

### III. DISCUSSION

#### A. Itinerant to local electronic transformation

Comparing magnetic and thermal properties one observes that, within the  $0 \leq y \leq 0.48$  range, this system presents an unusual discrepancy between the decreasing  $T_N(y)$  and the increasing amplitude of the  $\Delta C_m(T_N)$  jump, see Fig. 3a. The latter behavior is in line with the increasing values of magnetization presented in Fig. 2a. In an usual scenario of competing RKKY magnetic interactions with Kondo effect, the former mechanism tends to increase magnetic order whereas the later to screen magnetic mo-

ments [14]. This classical description does not apply to this system because a  $T_N(y)$  decrease would imply a weakening of the RKKY interaction due to an enhancement of the Kondo screening and the consequent decrease of  $\Delta C_m(T_N)$  [7]. On the contrary, the observed growing and narrowing of  $\Delta C_m(T_N)$  suggests a tendency towards the localization of Ce-4f states driven by a weakening of 4f-band hybridization (i.e. a decrease of  $T_K(y)$ ). Furthermore, the ferromagnetic type dependence of  $M(H)$  above  $H_{cr} \approx 0.5$  Tesla observed in the  $y \geq 0.48$  alloys clearly suggests a minor role of Kondo effect at this range of concentration. These facts make evident that different mechanisms are involved in the evolution of the ground state properties of this system.

The most likely is a decreasing contribution of the excited crystal electric field CEF levels at low energy, which leads the system into an itinerant to localized transformation. Taking into account that  $|\theta_P|$  can be considered  $\propto T_K$  [15], if  $|\theta_P|$  is comparable to the splitting  $\Delta_{CEF}$  of the first CEF level the contribution of that doublet is relevant, but it becomes irrelevant once  $|\theta_P| \ll \Delta_{CEF}$ . The reported decrease of  $|\theta_P|(y)$  from 58 K (at  $y = 0$ ) to 6 K (at  $y = 0.55$ ), together with the increase of  $\mu_{eff}$  and  $M(H)$  with concentration, support this description. From  $C_m(T)$  measurements up to  $T = 30$  K on sample  $y = 0.55$ , the first CEF splitting was evaluated as  $\Delta_{CEF} = 40 \pm 5$  K.

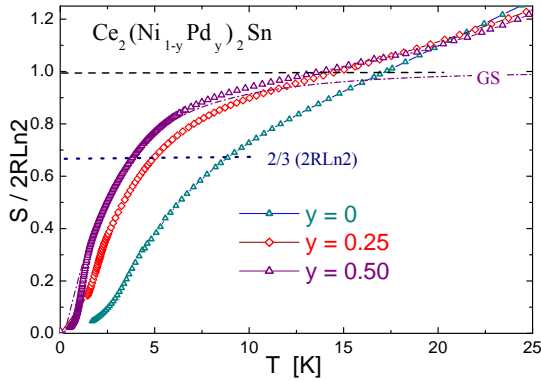


FIG. 5. Thermal dependence of the entropy (normalized to one Ce at.) for  $y = 0$  and the higher Pd concentrations. Dashed curve is a qualitative representation for the ground state contribution in sample  $y = 0.55$ .

An alternative way to test this scenario is the analysis of the entropy variation for different concentrations,  $S_m(y, T)$ . In Fig. 5 we show the thermal evolution of the magnetic entropy computed as  $S_m = \int C_m/T \times dT$ . On the Ni-rich limit, one sees that  $\text{Ce}_2\text{Ni}_2\text{Sn}$  presents a moderate and monotonous

increase of  $S_m(T)$  that overcomes  $S_m = 2R\ln 2$  around 15 K. This behavior reveals a significant broadening of ground and excited CEF levels that partially overlap each other because of comparable  $T_K$  and  $\Delta_{CEF}$  energies. On the contrary, the  $y = 0.50$  and  $0.55$  alloys show an incipient plateau of  $S_m(T)$  around  $T \geq 10$  K. This change confirms that the doublet GS is mostly occupied at that temperature whereas the first excited CFE doublet has reduced significantly its contribution to the GS properties. Applying Desgranges-Schotte [16] criterion of  $S_m(T_K) \simeq 2/3R\ln 2$  for single Kondo moments, the extracted values of  $T_K(y)$  clearly show a decrease of Ce-4f orbitals hybridization. This is the key to understand the unusual behavior of this system that can be explained as a combination between the decrease of the 4f-band hybridization intensity and the consequent reduction of the CFE levels contribution to the low energy density of states.

## B. Critical region and Phase Diagram

Another peculiarity of this system emerges from the analysis of the  $S_m(T)$  dependence at low temperature since the entropy gain at  $T_N$  is remarkably low, i.e.  $\approx 0.3R\ln 2$  per Ce-at. Such a low value is observed in Ce and Yb compounds which do not order because of e.g. magnetic frustration effects [17] but present a  $C_m(T)/T$  anomaly characterized by a divergent power law tail above the temperature of the maximum  $T_{max}$ . Although in  $\text{Ce}_2(\text{Pd}_{1-y}\text{Ni}_y)_2\text{Sn}$  the tail follows a  $-\log(T/T^*)$  dependence, the  $C_m/T$  maximum diverges at  $T_N(y)$  following a:  $5/(T-0.4) \text{ K}^{-1}$  dependence, as depicted in Fig. 4a, that should end in a critical point because of an *entropy bottleneck* [11]. This type of behavior was also observed in  $\text{URu}_2\text{Si}_2$  under magnetic field [18] and  $\text{CeTi}_y\text{Sc}_{1-y}\text{Ge}$  [19]. The latter shows a very similar divergency of its  $C_m/T$  maximum also approaching a structural instability.

In Fig. 4a and b one can see how the temperature of the magnetic anomaly decreases down to  $T_N \approx 1.2$  K at  $y_{cr} = 0.50$  where another contribution at  $T_I \approx 1.45$  K arises while the intensity of the former decreases. A detailed study of those specific heat anomalies around the critical region is presented in Fig. 6, performed at zero and applied magnetic field. Under magnetic field, the anomaly of the  $y_{cr} = 0.48$  alloy splits into two maxima. In that figure one can clearly see how the  $C_m/T$  maximum at  $T_N \approx 1.2$  K decreases in intensity while the one at  $T_I$  increases. The intrinsic character of this competition between a vanishing phase and an emerging one is confirmed by the same behavior observed in

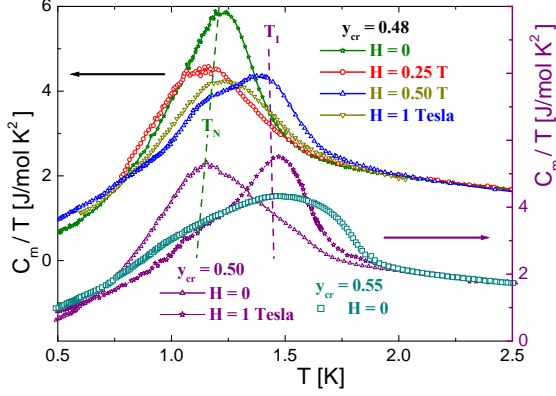


FIG. 6. Left axis (shifted up): specific heat of the magnetic anomaly of sample  $y_{cr} = 0.48$  at zero and three magnetic fields. Right axis: Comparison with other two concentrations. Dashed lines mark the mean temperatures of the anomalies at  $T_N \approx 1.2$  K and  $T_I \approx 1.5$  K.

the  $y = 0.50$  alloy, right axis in Fig. 6. Beyond that concentration, sample  $y = 0.55$  shows how the relative contributions are reversed. The growing intensity of the  $T_I$  anomaly with field and the  $M(H)$  dependence close to that temperature make evident a ferromagnetic character of this alloy despite of the lack of hysteresis in the  $M(H)$  curves.

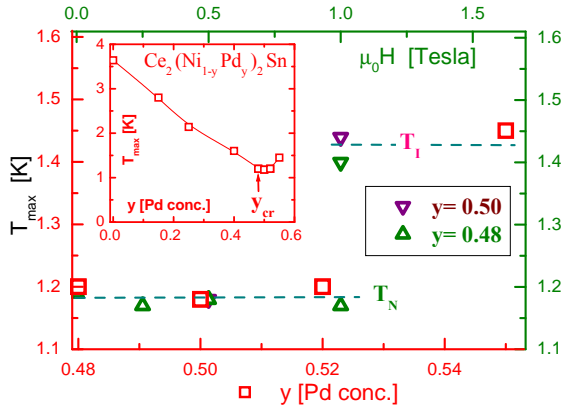


FIG. 7. Magnetic phase diagram around the critical point comparing  $T_N(0.48 \leq y \leq 0.55)$  ( $\square$ ) and field dependencies of  $y_{cr} = 0.48$  ( $\triangle$ ) and  $y = 0.50$  ( $\nabla$ ). Inset: full Pd concentration range for  $T_N(y)$ .

The overall concentration dependence of  $T_N(y)$  is included in the inset of Fig. 7, showing its decrease from 3.8 K down to 1.2 K at  $y_{cr} = 0.48$ . At that

concentration the competition between two phases occurs as it shown by specific heat measurements presented in Fig. 6. Those details are summarized in the main body of Fig. 7. There, concentration and magnetic field effects on both contributions with respective maxima at  $T_N \approx 1.2$  K and  $T_I \approx 1.45$  K are compared. Notice that thermal ( $k_B T_{max}$ ) and magnetic ( $\mu_B H$ ) energy scales used in the phase diagram are comparable.

#### IV. CONCLUSIONS

The outstanding characteristics observed in the  $\text{Ce}_2(\text{Ni}_{1-y}\text{Pd}_y)_2\text{Sn}$  family are the transformation of the magnetic properties from itinerant to mostly localized and the presence of a critical concentration with signatures of ferromagnetic contribution.

The former characteristic is recognized from the Pd concentration dependence of the magnetic properties like: i) the decrease of  $|\theta_P|$ , reflecting a decrease of  $T_K$ , ii) the increase of the effective magnetic moment and iii) the sharpening of the specific heat transition. All these properties behave at variance to the decrease of the ordering temperature  $T_N$  in a usual RKKY scenario of localized moments. In this system, the  $T_N(y)$  decrease is driven by the reduction of the CEF excited levels contribution to the ground state properties as revealed by the thermal evolution of the magnetic entropy with growing Pd concentration.

The second peculiarity of this system concerns the fact that the  $C_m(T)$  anomaly associated to  $T_N(y)$  shows a nearly constant maximum which ends into a *bottleneck* of the magnetic entropy at a critical concentration  $y_{cr} \approx 0.48$ . At that point  $M(H)$  reveals a ferromagnetic type dependence above  $H_{cr} \approx 0.4$  T. The splitting of the  $C_m(T)$  maximum, tuned by field and concentration indicates a competition between two magnetic phases within the  $0.48 \leq y \leq 0.55$  range. Their respective characteristic energies are  $T_N \approx 1.2$  K and  $T_I \approx 1.45$  K, with the former contribution vanishing and the latter arising as a function of concentration and/or field.

Lower temperature magnetic measurements (i.e.  $T < 1.8$  K) are required to better characterize the magnetic ground state within the critical region. Spectroscopic measurements may shed light into the dynamical nature of these competing phases and band calculations are highly desirable to trace the modification of the Fermi surface.

#### REFERENCES

- 
- [1] L.E. De Long, J.G. Huber and K.S. Bedell, *J. Magn. Magn. Mat* **99** (1991) 171.
  - [2] A.R. Mackintosh; *Physica* **130B** (1985) 112.
  - [3] See e.g. J.G. Sereni; *Physica B* **215** (1995) 273.
  - [4] S K Dhar, S K Malik and R Vijayaraghavan; *J. Phys. C: Solid State Phys.*, **14** (1981) L321-L324.
  - [5] S. Singh, S.K. Dahr, C. Mitra, P. Paulose, P. Manfrinetti, A. Palenzona; *J. Phys. Cond. Mat.* **13** (2001) 3753.
  - [6] See e.g. S. Kawarazaki, M. sato, Y. Miyako, N. Chigusa, K. Watamabe; *Phys. Rev. B* **61** (2000) 4167.
  - [7] J.G. Sereni, G. Schmerber, A. Braghta, B. Chevalier, J.P. Kappler; *arXiv* 1103.0190 cond-mat, 1 March 2011.
  - [8] F.J. DiSalvo, R.A. Gordon, C.M. Spencer, Y. Ijiri; *J. Alloys and Compd.* **224** (1995) 101.
  - [9] J.G. Sereni; *J. Low Temp. Phys.* **147** 179 (2007).
  - [10] H.v. Löhneysen, A. Rosch, M. Vojta, P. Wölfle, *Rew. Mod. Phys.* **79** (2007) 1015.
  - [11] J.G. Sereni; *Phil. Mag.* **93** (2013) 409.
  - [12] G.R. Stewart; *Rew. Mod. Phys.* **73** 797 (2001).
  - [13] J.G. Sereni, C. Geibel, M. G.-Berisso, P. Hellmann, O. Trovarelli and F. Steglich, *Physica B* **230** (1997) 580.
  - [14] M. Lavagna, C. Lacroix, M.J. Cyrot, *J. Phys. F* **12** (1982) 745.
  - [15] H.R. Krishna-murthy and C. Jayaprakash, *Phys. Rev. B* **30** (1984) 2806.
  - [16] H.-U. Desgranges and K.D. Schotte, *Physics Letters* **91A** 240 (1982).
  - [17] J.G. Sereni, 2014, to be published.
  - [18] M. Jaime, K.H. Kim, J. Guillermo, S. McCall, J.A. Mydosh; *Phys. Rev. Lett.*, **89** (2002) 287201.
  - [19] J.G. Sereni, P. Pedrazzini, M. Gmez Berisso, A. Chacoma, S. Encina, T. Gruner, N. Caroca-Canales, C. Geibel; *ArXiv:cond.mat* 1403.4490, 18 March 2014.